

Explaining $h \rightarrow \mu^\pm \tau^\mp$, $B \rightarrow K^* \mu^+ \mu^-$ and $B \rightarrow K \mu^+ \mu^- / B \rightarrow K e^+ e^-$ in a two-Higgs-doublet model with gauged $L_\mu - L_\tau$

Andreas Crivellin,¹ Giancarlo D'Ambrosio,^{1,2} and Julian Heeck³

¹*CERN Theory Division, CH-1211 Geneva 23, Switzerland*

²*INFN-Sezione di Napoli, Via Cintia, 80126 Napoli, Italy*

³*Service de Physique Théorique, Université Libre de Bruxelles,
 Boulevard du Triomphe, CP225, 1050 Brussels, Belgium*

The LHC observed so far three deviations from the Standard Model (SM) predictions in flavour observables: LHCb reported anomalies in $B \rightarrow K^* \mu^+ \mu^-$ and $R(K) = B \rightarrow K \mu^+ \mu^- / B \rightarrow K e^+ e^-$ while CMS found an excess in $h \rightarrow \mu \tau$. We show, for the first time, how these deviations from the SM can be explained within a single well-motivated model: a two-Higgs-doublet model with gauged $L_\mu - L_\tau$ symmetry. We find that, despite the constraints from $\tau \rightarrow \mu \mu \mu$ and $B_s - \bar{B}_s$ mixing, one can explain $h \rightarrow \mu \tau$, $B \rightarrow K^* \mu^+ \mu^-$ and $R(K)$ simultaneously, obtaining interesting correlations among the observables.

I. INTRODUCTION

So far, the LHC completed the SM by discovering the last missing piece, the Brout–Englert–Higgs particle [1, 2]. Furthermore, no significant direct evidence for physics beyond the SM has been found, i.e. no new particles were discovered. However, the LHC did observe three ‘hints’ for new physics (NP) in the flavor sector, which are sensitive to virtual effects of new particles and can be used as guidelines towards specific NP models: $h \rightarrow \mu \tau$, $B \rightarrow K^* \mu^+ \mu^-$, and $R(K) = B \rightarrow K \mu^+ \mu^- / B \rightarrow K e^+ e^-$. It is therefore interesting to examine if a specific NP model can explain these three anomalies simultaneously, predicting correlations among them.

LHCb reported deviations from the SM predictions [3, 4] (mainly in an angular observable called P'_5 [5]) in $B \rightarrow K^* \mu^+ \mu^-$ [6] with a significance of 2–3 σ depending on the assumptions of hadronic uncertainties [7–9]. This discrepancy can be explained in a model independent approach by rather large contributions to the Wilson coefficient C_9 [10–12], i.e. an operator $(\bar{s} \gamma_\alpha P_L b)(\bar{\mu} \gamma^\alpha \mu)$, which can be achieved in models with an additional heavy neutral Z' gauge boson [13–15]. Furthermore, LHCb [16] recently found indications for the violation of lepton flavour universality in

$$R(K) = \frac{B \rightarrow K \mu^+ \mu^-}{B \rightarrow K e^+ e^-} = 0.745^{+0.090}_{-0.074} \pm 0.036, \quad (1)$$

which disagrees from the theoretically rather clean SM prediction $R_K^{\text{SM}} = 1.0003 \pm 0.0001$ [17] by 2.6 σ . A possible explanation is again a NP contributing to $C_9^{\mu\mu}$ involving muons, but not electrons [18–20]. Interestingly, the value for C_9 required to explain $R(K)$ is of the same order as the one required by $B \rightarrow K^* \mu^+ \mu^-$ [8, 21]. In Ref. [15], a model with gauged muon minus tauon number ($L_\mu - L_\tau$) was proposed in order to explain the $B \rightarrow K^* \mu^+ \mu^-$ anomaly.

Concerning Higgs decays, CMS recently measured a lepton-flavour violating (LFV) channel [22]

$$\text{Br}[h \rightarrow \mu \tau] = (0.89^{+0.40}_{-0.37}) \%, \quad (2)$$

which disagrees from the SM (where this decay is forbidden) by about 2.4 σ . Such LFV SM Higgs couplings are

induced by a single operator up to dim-6 and $\text{Br}[h \rightarrow \mu \tau]$ can easily be up to 10% taking into account this operator only [23–28]. However, it is in general difficult to get dominant contributions to this operator in a UV complete model, as for example in models with vector-like leptons [29]. Therefore, among the several attempts to explain this $h \rightarrow \mu \tau$ observation [30–34], most of them are relying on models with extended Higgs sectors. One solution employs a two-Higgs-doublet model (2HDM) with gauged $L_\mu - L_\tau$ [35].

The abelian symmetry $U(1)_{L_\mu - L_\tau}$ is interesting in general: not only is this an anomaly-free global symmetry within the SM [36–38], it is also a good zeroth-order approximation for neutrino mixing with a quasi-degenerate mass spectrum, predicting a maximal atmospheric and vanishing reactor neutrino mixing angle [39–41]. Breaking $L_\mu - L_\tau$ is mandatory for a realistic neutrino sector, and such a breaking can also induce charged LFV processes, such as $\tau \rightarrow 3\mu$ [42, 43] and $h \rightarrow \mu \tau$ [35].

Supplementing the model of Ref. [35] with the induced Z' quark couplings of Ref. [15] can resolve all three anomalies from above. Interestingly, the semileptonic B decays imply lower limit on $g'/M_{Z'}$, which allows us to set a lower limit on $\tau \rightarrow \mu \mu \mu$, depending on $h \rightarrow \mu \tau$.

II. THE MODEL

Our model under consideration is a 2HDM with a gauged $U(1)_{L_\mu - L_\tau}$ symmetry [35]. The $L_\mu - L_\tau$ symmetry with the gauge coupling g' is broken spontaneously by the vacuum expectation value (VEV) of a scalar Φ with $Q_{L_\mu - L_\tau}^\Phi = 1$, leading to the Z' mass

$$m_{Z'} = \sqrt{2} g' \langle \Phi \rangle \equiv g' v_\Phi, \quad (3)$$

and Majorana masses for the right-handed neutrinos¹.

Two Higgs doublets are introduced which break the electroweak symmetry: Ψ_1 with $Q_{L_\mu - L_\tau}^{\Psi_1} = -2$ and Ψ_2

¹ Active neutrino masses are generated via seesaw with close-to-maximal atmospheric mixing and quasi-degenerate masses [35].

with $Q_{L_\mu-L_\tau}^{\Psi_2} = 0$. Therefore, Ψ_2 gives masses to quarks and leptons while Ψ_1 couples only off-diagonally to $\tau\mu$:

$$\begin{aligned} \mathcal{L}_Y \supset & -\bar{\ell}_f Y_i^\ell \delta_{fi} \Psi_2 e_i - \xi_{\tau\mu} \bar{\ell}_3 \Psi_1 e_2 \\ & - \bar{Q}_f Y_{f_i}^u \tilde{\Psi}_2 u_i - \bar{Q}_f Y_{f_i}^d \Psi_2 d_i + \text{h.c.} \end{aligned} \quad (4)$$

Here Q (ℓ) is the left-handed quark (lepton) doublet, u (e) is the right-handed up-quark (charged-lepton) and d the right-handed down quark while i and f label the three generations. The scalar potential is the one of a $U(1)$ -invariant 2HDM [44] with additional couplings to the SM-singlet Φ , which most importantly generates the doublet-mixing term

$$V(\Psi_1, \Psi_2, \Phi) \supset 2\lambda\Phi^2\Psi_2^\dagger\Psi_1 \rightarrow \lambda v_\Phi^2\Psi_2^\dagger\Psi_1 \equiv m_3^2\Psi_2^\dagger\Psi_1,$$

that induces a small vacuum expectation value for Ψ_1 [35]. We define $\tan\beta = \langle\Psi_2\rangle/\langle\Psi_1\rangle$ and α is the usual mixing angle between the neutral CP-even components of Ψ_1 and Ψ_2 (see for example [44]). We neglect the additional mixing of the CP-even scalars with $\text{Re}[\Phi]$.

Quarks and gauge bosons have standard type-I 2HDM couplings to the scalars. The only deviations are in the lepton sector: while the Yukawa couplings $Y_i^\ell\delta_{fi}$ of Ψ_2 are forced to be diagonal due to the $L_\mu - L_\tau$ symmetry, $\xi_{\tau\mu}$ gives rise to an off-diagonal entry in the lepton mass matrix:

$$m_{fi}^\ell = \frac{v}{\sqrt{2}} \begin{pmatrix} y_e \sin\beta & 0 & 0 \\ 0 & y_\mu \sin\beta & 0 \\ 0 & \xi_{\tau\mu} \cos\beta & y_\tau \sin\beta \end{pmatrix}. \quad (5)$$

It is this τ - μ entry that leads to the LFV couplings of h and Z' of interest to this letter. The lepton mass basis is obtained by simple rotations of (μ_R, τ_R) and (μ_L, τ_L) with the angles θ_R and θ_L , respectively:

$$\sin\theta_R \simeq \frac{v}{\sqrt{2}m_\tau} \xi_{\tau\mu} \cos\beta, \quad \frac{\tan\theta_L}{\tan\theta_R} = \frac{m_\mu}{m_\tau} \ll 1. \quad (6)$$

The angle θ_L is automatically small and will be neglected in the following.² A non-vanishing angle θ_R not only gives rise to the LFV decay $h \rightarrow \mu\tau$ due to the coupling

$$\frac{m_\tau}{v} \frac{\cos(\alpha-\beta)}{\cos(\beta)\sin(\beta)} \sin(\theta_R) \cos(\theta_R) \bar{\tau} P_R \mu h \equiv \Gamma_{\tau\mu}^h \bar{\tau} P_R \mu h, \quad (7)$$

in the Lagrangian, but also leads to off-diagonal Z' couplings to right-handed leptons

$$g' Z'_\nu (\bar{\mu}, \bar{\tau}) \begin{pmatrix} \cos 2\theta_R & \sin 2\theta_R \\ \sin 2\theta_R & -\cos 2\theta_R \end{pmatrix} \gamma^\nu P_R \begin{pmatrix} \mu \\ \tau \end{pmatrix}, \quad (8)$$

while the left-handed couplings are to a good approximation flavour conserving. In order to explain the observed anomalies in the B meson decays, a coupling of the Z' to quarks is required as well, not inherently part of $L_\mu - L_\tau$

models (aside from the kinetic Z - Z' mixing, which is assumed to be small). Following Ref. [15], we introduce heavy vector-like quarks, i.e. $Q_L \equiv (U_L, D_L)$, D_R^c , U_R^c and their chiral partners $\tilde{Q}_R \equiv (\tilde{U}_R, \tilde{D}_R)$, \tilde{D}_L^c , \tilde{U}_L^c , with vector-like mass terms

$$m_Q \bar{Q}_L \tilde{Q}_R + m_D \bar{\tilde{D}}_L D_R + m_U \bar{\tilde{U}}_L U_R + \text{h.c.}, \quad (9)$$

and $L_\mu - L_\tau$ charges $+1$ (i.e. $Q_{L_\mu-L_\tau}^{D_R} = Q_{L_\mu-L_\tau}^{U_R} = -1$), coupling them to the Z' boson. Yukawa-like couplings involving the heavy vector-quarks, the light chiral quarks and Φ

$$\begin{aligned} \Phi \sum_{j=1}^3 \left(\bar{\tilde{D}}_R Y_j^Q P_L d_j + \bar{\tilde{U}}_R Y_j^Q P_L u_j \right) \\ + \Phi^\dagger \sum_{j=1}^3 \left(\bar{\tilde{D}}_L Y_j^D P_R d_j + \bar{\tilde{U}}_L Y_j^U P_R u_j \right) + \text{h.c.} \end{aligned} \quad (10)$$

then induce couplings of the SM quarks to the Z' once Φ acquires its VEV. Thus, integrating out the heavy vector-like quarks gives rise to effective $Z'\bar{d}_i d_j$ couplings [45, 46] of the form

$$g' (\bar{d}_i \gamma^\mu P_L d_j Z'_\mu \Gamma_{ij}^{dL} + \bar{d}_i \gamma^\mu P_R d_j Z'_\mu \Gamma_{ij}^{dR}), \quad (11)$$

with hermitian matrices Γ_{ij}^{dL} that are related to the vector quark masses $m_{Q,D,U}$ and Yukawa couplings $Y^{Q,D,U}$ as follows [15]:

$$\Gamma_{ij}^{dR} \simeq -\frac{v_\Phi^2}{2m_D^2} (Y_i^D Y_j^{D*}), \quad \Gamma_{ij}^{dL} \simeq \frac{v_\Phi^2}{2m_Q^2} (Y_i^Q Y_j^{Q*}), \quad (12)$$

which holds in the approximation $|\Gamma_{ij}^{qR/L}| \ll 1$.³

III. FLAVOUR OBSERVABLES

We will now recall the necessary formula in the region of interest (i.e. small θ_R) considering only the processes giving to most relevant bounds on our model, i.e. $B_s-\bar{B}_s$ mixing, neutrino trident production and $\tau \rightarrow 3\mu$.

A. $h \rightarrow \mu\tau$

The branching ratio for $h \rightarrow \mu\tau$ reads

$$\text{Br}[h \rightarrow \mu\tau] \simeq \frac{m_h}{8\pi\Gamma_{\text{SM}}} |\Gamma_{\tau\mu}^h|^2, \quad (13)$$

where $\Gamma_{\text{SM}} \simeq 4.1 \text{ MeV}$ is the decay width in the SM for a 125 GeV Higgs [47] and $\Gamma_{\tau\mu}^h$ is defined in Eq. (7). Comparing this to Eq. (2) one sees that both $\sin\theta_R \neq 0$ and $\cos(\alpha-\beta) \neq 0$ are required to explain the CMS excess [35].

² Choosing $Q_{L_\mu-L_\tau} = +2$ for Ψ_2 would essentially exchange $\theta_L \leftrightarrow \theta_R$ [35], with little impact on our study.

³ Compared to Ref. [15], the vector-like quarks also have Yukawa couplings y_{Ψ_1} to the $L_\mu - L_\tau$ -charged scalar doublet Ψ_1 . This induces a small additional mass mixing among the heavy quarks, and also a coupling to h suppressed by $y_{\Psi_1} \cos(\alpha-\beta)$. We assume these couplings y_{Ψ_1} to be small to avoid large contributions to $g\gamma \rightarrow h$ and $h \rightarrow \gamma\gamma$.

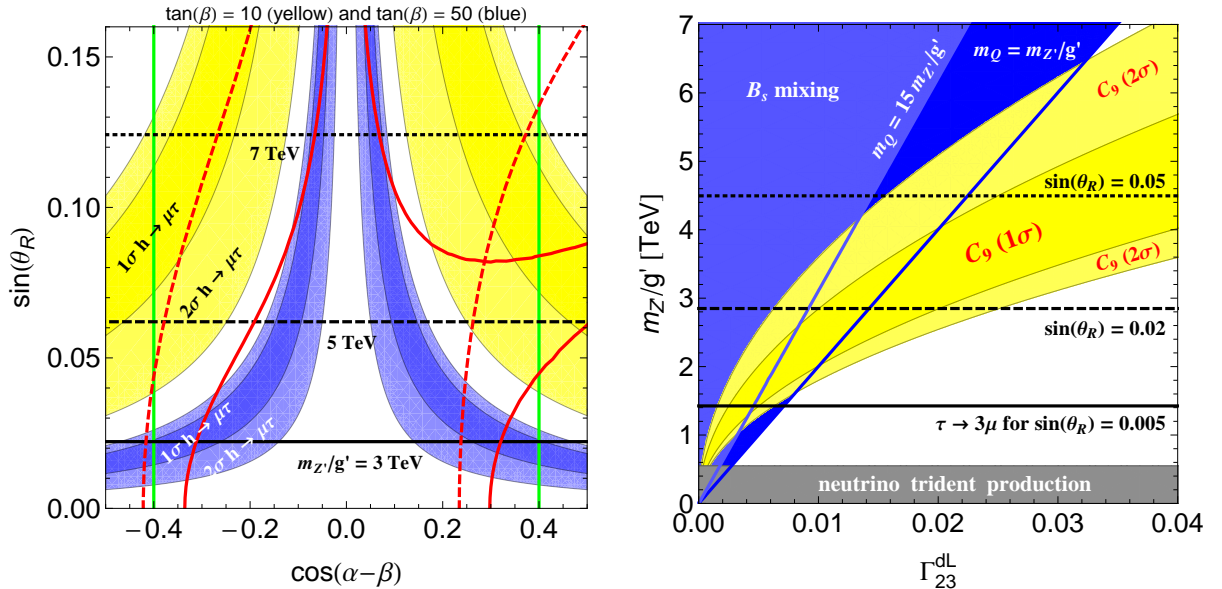


FIG. 1: Left: Allowed regions in the $\cos(\alpha - \beta)$ – $\sin(\theta_R)$ plane. The blue (light blue) region corresponds to the 1σ (2σ) region of the CMS measurement of $h \rightarrow \mu\tau$ for $\tan\beta = 50$; yellow stands for $\tan\beta = 10$. The (dashed) red contours mark deviations of $h \rightarrow \tau\tau$ by 10% compared to the SM for $\tan\beta = 50$ (10). The vertical green lines illustrate the naive LHC limit $|\cos(\alpha - \beta)| \lesssim 0.4$, horizontal lines denote the 90% C.L. limit on $\tau \rightarrow 3\mu$ via Z' exchange.

Right: Allowed regions in the Γ_{23}^{dL} – $m_{Z'}/g'$ plane from $B \rightarrow K^*\mu^+\mu^-$ and $R(K)$ (yellow) and B_s mixing (blue). For B_s mixing (light) blue corresponds to $(m_Q = 15m_{Z'}/g')$ $m_Q = m_{Z'}/g'$. The horizontal lines denote the lower bounds on $m_{Z'}/g'$ from $\tau \rightarrow 3\mu$ for $\sin(\theta_R) = 0.05, 0.02, 0.005$. The gray region is excluded by NTP.

B. Lepton decays

While the Higgs contributions to $\tau \rightarrow \mu\mu\mu$ and $\tau \rightarrow \mu\gamma$ turn out to be very small in most regions of parameter space [35] due to the small lepton masses involved, the Z' contributions to $\tau \rightarrow 3\mu$ can be sizable [42] and restrict θ_R^2/v_Φ^4 . The branching ratio is given by

$$\text{Br}[\tau \rightarrow 3\mu] \simeq \frac{m_\tau^5}{512\pi^3\Gamma_\tau} \frac{g'^4}{m_{Z'}^4} \sin^2(2\theta_R), \quad (14)$$

which has to be compared to the current upper limit of 2.1×10^{-8} at 90% C.L. [48] obtained by Belle. A combination with data from BaBar [49] gives an even stronger limit of 1.2×10^{-8} at 90% C.L. [50], to be used in the following. For small θ_R , the branching ratio for $\tau \rightarrow \mu\gamma$ is proportional to the same combination θ_R^2/v_Φ^4 , but highly suppressed by $2\alpha/\pi$, and hence not as restrictive.

C. $B \rightarrow K^*\mu^+\mu^-$ and $B \rightarrow K\mu^+\mu^-/B \rightarrow Ke^+e^-$

Both $B \rightarrow K^*\mu^+\mu^-$ and $R(K)$ are sensitive to the Wilson coefficients $C_9^{(\prime)\mu\mu}$ and $C_{10}^{(\prime)\mu\mu}$.⁴ While in our model the contribution to C_{10} is suppressed by $\sin(2\theta_R)$ (or even $\sin(2\theta_L)$), the Wilson coefficients $C_9^{\mu\mu}$ and $C_9^{\prime\mu\mu}$ with muons are generated (as well as $C_9^{\tau\tau}$ and the θ_R

suppressed $C_9^{\mu\tau}$). C_9^{tee} is not affected, which naturally generates violations of lepton flavour universality in $B \rightarrow K\mu^+\mu^-/B \rightarrow Ke^+e^-$. We find

$$C_9^{(\prime)\mu\mu} \simeq \frac{g'^2}{\sqrt{2}m_{Z'}^2} \frac{\pi}{\alpha} \frac{1}{G_F V_{tb} V_{ts}^*} \Gamma_{23}^{dL(R)}, \quad (15)$$

where we set $\cos(2\theta_R) = 1$. As already noted in Ref. [10, 51] $C_9^{\mu\mu} < 0$ and $C_9^{\prime\mu\mu} = 0$ gives a good fit to data. Using the global fit of Ref. [8] we see that at (1σ) 2σ level

$$-0.5(-0.8) \geq \text{Re} C_9^{\mu\mu} \geq (-1.6) - 2.0. \quad (16)$$

Interestingly, the regions for $C_9^{\mu\mu}$ required by $R(K)$ and $B \rightarrow K^*\mu^+\mu^-$ lie approximately in the same region. Furthermore, a good fit to the current data does not even require $C_9^{\prime\mu\mu}$ [8], so we neglect it in the following for simplicity. This can be achieved in the limit $m_D \gg m_Q$, resulting in $\Gamma^{dL} \gg \Gamma^{dR}$. We will also assume our $C_9^{\mu\mu}$ to be real for simplicity. Note that our model predicts the decay $B \rightarrow K\mu\tau$ (recently discussed in Refs. [52]) to be suppressed by θ_R^2 compared to $B \rightarrow K\mu\mu$, while $B \rightarrow K\mu e$ and $B \rightarrow K\tau e$ are forbidden.

D. B_s – \bar{B}_s mixing

The interactions of Z' and Φ relevant for $B \rightarrow K\mu^+\mu^-$ also contribute to B_s – \bar{B}_s mixing [15]. For $m_D \gg m_Q$,

⁴ For conventions see Refs. [8, 19].

we get

$$\frac{M_{12}}{M_{12}^{\text{SM}}} \simeq 1 + \frac{(\Gamma_{23}^{dL})^2 \left(1 + \frac{1}{16\pi^2} \frac{g'^2 m_Q^2}{m_{Z'}^2}\right)}{\frac{g_s^4}{64\pi^2} \frac{m_{Z'}^2}{m_W^2 g'^2} (V_{ts}^* V_{tb})^2 S_0}. \quad (17)$$

We require the NP contribution to be less than 15% in order to satisfy the experimental bounds [15]. Due to the dominance of the vector-quark Q we can express Γ_{23}^{dL} directly in terms of $C_9^{\mu\mu}$ from Eq. (15) and find the *upper* bounds

$$m_{Z'}/g' < 3.2 \text{ TeV}/|C_9^{\mu\mu}|, \quad m_Q < 41 \text{ TeV}/|C_9^{\mu\mu}|. \quad (18)$$

Combining Eq. (18) with Eq. (16) then gives an upper bound of $m_{Z'}/g' < 4 \text{ TeV}$ (6.5 TeV) at 1σ (2σ).

E. Neutrino trident production

The most stringent bound on flavour-diagonal Z' couplings to muons arises from neutrino trident production (NTP) $\nu_\mu N \rightarrow \nu_\mu N \mu^+ \mu^-$ [15, 53]:

$$\frac{\sigma_{\text{NTP}}}{\sigma_{\text{NTP}}^{\text{SM}}} \simeq \frac{1 + \left(1 + 4s_W^2 + 8 \frac{g'^2}{M_{Z'}^2} \frac{m_W^2}{g_2^2}\right)^2}{1 + (1 + 4s_W^2)^2}. \quad (19)$$

Seeing as our region of interest is in the small θ_R regime, the NTP bound is basically independent of the angle θ_R . Taking only the CCFR data [54], we get roughly $m_{Z'}/g' \gtrsim 550 \text{ GeV}$ at 95% C.L. Compared to $\tau \rightarrow \mu\mu\mu$ the trident neutrino bound only dominates for very small values of θ_R , roughly when $\theta_R \lesssim 10^{-3}$ (see Fig. 2 (right)).

For $m_{Z'} > m_Z$, the LHC constraints from the process $pp \rightarrow \mu\mu Z' \rightarrow 4\mu$ (or 3μ plus missing energy) [55] are currently weaker than NTP [15], but will become competitive with higher luminosities [56–58].

F. Phenomenological analysis

Concerning the phenomenological consequences of of our model, let us first consider the implications of $h \rightarrow \mu\tau$. In the left plot of Fig. 1 we show the regions in the $\cos(\alpha - \beta)$ – $\sin(\theta_R)$ plane which can explain $h \rightarrow \mu\tau$ at the 1σ and 2σ level for different values of $\tan\beta$. Measurements of the h couplings to vector bosons require $|\cos(\alpha - \beta)| \lesssim 0.4$ [59, 60] while the Higgs effects in $\tau \rightarrow 3\mu$ and $\tau \rightarrow \mu\gamma$ are typically negligible [35]. As a side effect, the $h \rightarrow \mu\tau$ rate also implies a change in the $h \rightarrow \tau\tau$ rate, although this is negligible in regions with small θ_R . In addition we show the regions compatible with $\tau \rightarrow 3\mu$ for various values of $m_{Z'}/g'$. Note that $g' \lesssim 0.3$ in order to avoid a Landau pole below the Planck scale. In summary, small values of θ_R can explain the CMS $h \rightarrow \mu\tau$ excess for moderate to large values of $\tan\beta$ for $\cos(\alpha - \beta) \simeq 0.1$.

In the right plot of Fig. 1 we examine which regions in parameter space can account for $B \rightarrow K^* \mu^+ \mu^-$ taking into account the constraints from $B_s - \bar{B}_s$ mixing. Since

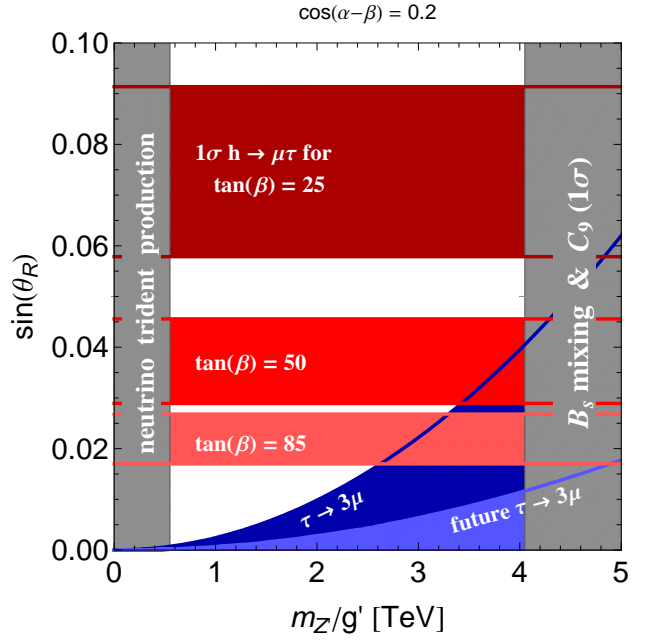


FIG. 2: Allowed regions in the $m_{Z'}/g'$ – $\sin(\theta_R)$ plane: the horizontal stripes correspond to $h \rightarrow \mu\tau$ (1σ) for $\tan\beta = 85, 50, 25$ and $\cos(\alpha - \beta) = 0.2$, (light) blue stands for (future) $\tau \rightarrow 3\mu$ limits at 90% C.L. The gray regions are excluded by NTP or $B_s - \bar{B}_s$ mixing in combination with the 1σ range for C_9 (see Eq. (18)).

we focus on the limit $M_D \rightarrow \infty$ (i.e. $C_9' \rightarrow 0$) we find that unless Γ_{23}^{dL} is rather large, $B \rightarrow K^* \mu^+ \mu^-$ can be explained without violating bounds from $B_s - \bar{B}_s$. Only a very small Γ_{23}^{dL} independent region is excluded by NTP. In addition, bounds from $\tau \rightarrow 3\mu$ depending on $\sin(\theta_R)$ can be obtained.

Concerning $\tau \rightarrow 3\mu$, future sensitivities down to $\text{Br}[\tau \rightarrow 3\mu] \simeq 10^{-9}$ seem feasible [61] and will cut deep into our parameter space (see Fig. 2). Using the 1σ limits on $h \rightarrow \mu\tau$ to fix θ_R and B_s mixing with C_9 to fix $m_{Z'}/g'$ – as well as the LHC limit $|\cos(\alpha - \beta)| < 0.4$ – we can obtain a *lower* limit on the rate $\tau \rightarrow 3\mu$

$$\text{Br}[\tau \rightarrow 3\mu] \gtrsim 3.8 \times 10^{-8} (10/\tan\beta)^2, \quad (20)$$

which implies $\tan\beta \gtrsim 18$ with current data [50] and $\tan\beta \gtrsim 61$ if branching ratios down to 10^{-9} can be probed in the future. This is the main prediction of our simultaneous explanation of $h \rightarrow \mu\tau$, $B \rightarrow K^* \mu^+ \mu^-$ and $R(K)$.

Finally, we remark that a Z – Z' mixing angle $\theta_{ZZ'}$ [45] is induced by the VEV of Ψ_1 [35]

$$|g'\theta_{ZZ'}| \simeq \frac{g_1 v^2 \cos^2 \beta}{m_{Z'}^2 / g'^2} \simeq 10^{-4} \left(\frac{20}{\tan\beta}\right)^2 \left(\frac{\text{TeV}}{m_{Z'}/g'}\right)^2, \quad (21)$$

which leads to small shifts in the vector couplings of Z to muons and taus

$$g_V^Z(\mu\mu, \tau\tau) \simeq -1/2 + 2s_W^2 \pm g'\theta_{ZZ'}/(g/c_W), \quad (22)$$

and thus ultimately to lepton non-universality [43]. For the values of interest to our study (see Fig. 2), and in

the limit $m_Z \ll m_{Z'}$, the shift is automatically small enough to satisfy experimental bounds and leads to tiny branching ratios $Z \rightarrow \mu\tau$ below 10^{-8} (for $\theta_R < 0.1$). Note that the couplings to electrons and quarks remain unaffected. For $m_{Z'} \gg m_Z$, the ρ parameter is enhanced by [45]

$$\rho - 1 \simeq 1.2 \times 10^{-4} \left(\frac{\theta_{ZZ'}}{10^{-3}} \right)^2 \left(\frac{m_{Z'}}{\text{TeV}} \right)^2, \quad (23)$$

and is therefore compatible with electroweak precision data ($\rho - 1 < 9 \times 10^{-4}$ at 2σ [62]) for the parameter space studied in this letter.

IV. CONCLUSIONS

In this letter we showed for the first time that all three LHC anomalies in the flavour sector can be explained within a single well-motivated model: A 2HDM with a gauged $L_\mu - L_\tau$ symmetry and effective $Z' \bar{s}b$ couplings induced by heavy vector-like quarks. Except for the $\tau - \mu$ couplings, the Higgs sector resembles the one of a 2HDM of type-I. Therefore, the constraints from h decays or LHC searches for $A^0 \rightarrow \tau^+\tau^-$ are rather weak and $h \rightarrow \mu\tau$ can be easily explained in a wide parameter space. The model can also account for the deviations from the SM in $B \rightarrow K^* \mu^+ \mu^-$ and naturally leads to the right amount of lepton-flavour-universality violating effects in $R(K)$. Due to the small values of the $\tau - \mu$ mixing angle θ_R , sufficient to account for $h \rightarrow \mu\tau$, the Z' contributions to $\tau \rightarrow 3\mu$ are not in conflict with

present bounds for large $\tan\beta$ in wide ranges of parameter space. Interestingly, $B \rightarrow K^* \mu^+ \mu^-$ and $R(K)$ combined with $B_s - \bar{B}_s$ put an upper limit on $m_{Z'}/g'$ resulting in a lower limit on $\tau \rightarrow 3\mu$ if $\text{Br}[h \rightarrow \mu\tau] \neq 0$: for lower values of $\tan\beta$ the current experimental bounds are reached and future sensitivities will allow for a more detailed exploration of the allowed parameter space. The possible range for the $L_\mu - L_\tau$ breaking scale further implies the masses of the Z' and the right-handed neutrinos to be at the TeV scale, potentially testable at the LHC with interesting additional consequences for LFV observables.

Acknowledgments

A. Crivellin is supported by a Marie Curie Intra-European Fellowship of the European Community's 7th Framework Programme under contract number PIEF-GA-2012-326948. G. D'Ambrosio acknowledges the partial support my MIUR under the project number 2010YJ2NYW. The work of J. Heeck is funded in part by IISN and by Belgian Science Policy (IAP VII/37). We thank Gian Giudice for useful discussions. We are grateful to Wolfgang Altmannshofer and David Straub for useful discussions and additional information concerning the model-independent fit to $C_9^{\mu\mu}$ and $C_9^{\prime\mu\mu}$.

Note added: during the publication process of this letter, CMS has released its final analysis of the $h \rightarrow \mu\tau$ search as a preprint [63], resulting in slightly changed values $-\text{Br}[h \rightarrow \mu\tau] = (0.84_{-0.37}^{+0.39})\%$ – which have however only a small impact on our study.

-
- [1] G. Aad et al. (ATLAS Collaboration), Phys.Lett. **B716**, 1 (2012), 1207.7214.
- [2] S. Chatrchyan et al. (CMS Collaboration), Phys.Lett. **B716**, 30 (2012), 1207.7235.
- [3] U. Egede, T. Hurth, J. Matias, M. Ramon, and W. Reece, JHEP **0811**, 032 (2008), 0807.2589.
- [4] W. Altmannshofer, P. Ball, A. Bharucha, A. J. Buras, D. M. Straub, et al., JHEP **0901**, 019 (2009), 0811.1214.
- [5] S. Descotes-Genon, T. Hurth, J. Matias, and J. Virto, JHEP **1305**, 137 (2013), 1303.5794.
- [6] R. Aaij et al. (LHCb collaboration), Phys.Rev.Lett. **111**, 191801 (2013), 1308.1707.
- [7] S. Descotes-Genon, L. Hofer, J. Matias, and J. Virto, JHEP **1412**, 125 (2014), 1407.8526.
- [8] W. Altmannshofer and D. M. Straub (2014), 1411.3161.
- [9] S. Jäger and J. Martin Camalich (2014), 1412.3183.
- [10] S. Descotes-Genon, J. Matias, and J. Virto, Phys.Rev. **D88**, 074002 (2013), 1307.5683.
- [11] W. Altmannshofer and D. M. Straub, Eur.Phys.J. **C73**, 2646 (2013), 1308.1501.
- [12] R. R. Horgan, Z. Liu, S. Meinel, and M. Wingate, Phys.Rev.Lett. **112**, 212003 (2014), 1310.3887.
- [13] R. Gauld, F. Goertz, and U. Haisch, Phys.Rev. **D89**, 015005 (2014), 1308.1959.
- [14] A. J. Buras, F. De Fazio, and J. Girrbach, JHEP **1402**, 112 (2014), 1311.6729.
- [15] W. Altmannshofer, S. Gori, M. Pospelov, and I. Yavin, Phys.Rev. **D89**, 095033 (2014), 1403.1269.
- [16] R. Aaij et al. (LHCb collaboration), Phys.Rev.Lett. **113**, 151601 (2014), 1406.6482.
- [17] C. Bobeth, G. Hiller, and G. Piranishvili, JHEP **0712**, 040 (2007), 0709.4174.
- [18] R. Alonso, B. Grinstein, and J. Martin Camalich, Phys.Rev.Lett. **113**, 241802 (2014), 1407.7044.
- [19] G. Hiller and M. Schmaltz, Phys.Rev. **D90**, 054014 (2014), 1408.1627.
- [20] D. Ghosh, M. Nardecchia, and S. Renner, JHEP **1412**, 131 (2014), 1408.4097.
- [21] T. Hurth, F. Mahmoudi, and S. Neshatpour, JHEP **1412**, 053 (2014), 1410.4545.
- [22] CMS (CMS Collaboration) (2014), CMS-PAS-HIG-14-005.
- [23] R. Harnik, J. Kopp, and J. Zupan, JHEP **1303**, 026 (2013), 1209.1397.
- [24] G. Blankenburg, J. Ellis, and G. Isidori, Phys.Lett. **B712**, 386 (2012), 1202.5704.
- [25] S. Davidson and P. Verdier, Phys.Rev. **D86**, 111701 (2012), 1211.1248.
- [26] A. Arhrib, Y. Cheng, and O. C. Kong, Phys.Rev. **D87**, 015025 (2013), 1210.8241.
- [27] A. Arhrib, Y. Cheng, and O. C. Kong, Europhys.Lett. **101**, 31003 (2013), 1208.4669.
- [28] J. Kopp and M. Nardecchia, JHEP **1410**, 156 (2014), 1406.5303.

- [29] A. Falkowski, D. M. Straub, and A. Vicente, *JHEP* **1405**, 092 (2014), 1312.5329.
- [30] A. Dery, A. Efrati, Y. Nir, Y. Soreq, and V. Susi, *Phys.Rev.* **D90**, 115022 (2014), 1408.1371.
- [31] M. D. Campos, A. E. C. Hernández, H. Päs, and E. Schumacher (2014), 1408.1652.
- [32] A. Celis, V. Cirigliano, and E. Passemar (2014), 1409.4439.
- [33] D. Aristizabal Sierra and A. Vicente, *Phys.Rev.* **D90**, 115004 (2014), 1409.7690.
- [34] C.-J. Lee and J. Tandean (2014), 1410.6803.
- [35] J. Heeck, M. Holthausen, W. Rodejohann, and Y. Shimizu (2014), 1412.3671.
- [36] X. He, G. C. Joshi, H. Lew, and R. Volkas, *Phys.Rev.* **D43**, 22 (1991).
- [37] R. Foot, *Mod.Phys.Lett.* **A6**, 527 (1991).
- [38] X.-G. He, G. C. Joshi, H. Lew, and R. Volkas, *Phys.Rev.* **D44**, 2118 (1991).
- [39] P. Binetruy, S. Lavignac, S. T. Petcov, and P. Ramond, *Nucl.Phys.* **B496**, 3 (1997), hep-ph/9610481.
- [40] N. F. Bell and R. R. Volkas, *Phys.Rev.* **D63**, 013006 (2001), hep-ph/0008177.
- [41] S. Choubey and W. Rodejohann, *Eur.Phys.J.* **C40**, 259 (2005), hep-ph/0411190.
- [42] G. Dutta, A. S. Joshipura, and K. Vijaykumar, *Phys.Rev.* **D50**, 2109 (1994), hep-ph/9405292.
- [43] J. Heeck and W. Rodejohann, *Phys.Rev.* **D84**, 075007 (2011), 1107.5238.
- [44] G. Branco, P. Ferreira, L. Lavoura, M. Rebelo, M. Sher, et al., *Phys.Rept.* **516**, 1 (2012), 1106.0034.
- [45] P. Langacker, *Rev.Mod.Phys.* **81**, 1199 (2009), 0801.1345.
- [46] A. J. Buras, F. De Fazio, and J. Girrbach, *JHEP* **1302**, 116 (2013), 1211.1896.
- [47] S. Dittmaier, S. Dittmaier, C. Mariotti, G. Passarino, R. Tanaka, et al. (2012), 1201.3084.
- [48] B. Aubert et al. (BaBar Collaboration), *Phys.Rev.Lett.* **104**, 021802 (2010), 0908.2381.
- [49] J. Lees et al. (BaBar Collaboration), *Phys.Rev.* **D81**, 111101 (2010), 1002.4550.
- [50] Y. Amhis et al. (Heavy Flavor Averaging Group (HFAG)) (2014), 1412.7515.
- [51] S. Descotes-Genon, J. Matias, and J. Virto, *PoS EPS-HEP2013*, 361 (2013), 1311.3876.
- [52] S. L. Glashow, D. Guadagnoli, and K. Lane (2014), 1411.0565.
- [53] W. Altmannshofer, S. Gori, M. Pospelov, and I. Yavin, *Phys.Rev.Lett.* **113**, 091801 (2014), 1406.2332.
- [54] S. Mishra et al. (CCFR Collaboration), *Phys.Rev.Lett.* **66**, 3117 (1991).
- [55] E. Ma, D. Roy, and S. Roy, *Phys.Lett.* **B525**, 101 (2002), hep-ph/0110146.
- [56] K. Harigaya, T. Igari, M. M. Nojiri, M. Takeuchi, and K. Tobe, *JHEP* **1403**, 105 (2014), 1311.0870.
- [57] N. F. Bell, Y. Cai, R. K. Leane, and A. D. Medina, *Phys.Rev.* **D90**, 035027 (2014), 1407.3001.
- [58] F. del Aguila, M. Chala, J. Santiago, and Y. Yamamoto (2014), 1411.7394.
- [59] B. Dumont, J. F. Gunion, Y. Jiang, and S. Kraml, *Phys.Rev.* **D90**, 035021 (2014), 1405.3584.
- [60] B. Dumont, J. F. Gunion, Y. Jiang, and S. Kraml (2014), 1409.4088.
- [61] T. Aushev, W. Bartel, A. Bondar, J. Brodzicka, T. Browder, et al. (2010), 1002.5012.
- [62] K. Olive et al. (Particle Data Group), *Chin.Phys.* **C38**, 090001 (2014).
- [63] V. Khachatryan et al. (CMS Collaboration) (2015), 1502.07400.